Available online at www.sciencedirect.com
SCIENCE DIRECT
Journal of Solid State Chemistry 179 (2006) 985–992
JOURNAL OF SOLID STATE CHEMISTRY
www.elsevier.com/locate/jssc

Photoluminescence in disordered Zn_2TiO_4

Alexsandra C. Chaves[a], Severino J.G. Lima[b], Regiane C.M.U. Araújo[a], Maria Aldeiza M.A. Maurera[a], Elson Longo[c], Paulo S. Pizani[d], Luiz G.P. Simões[c], Luiz E.B. Soledade[a], Antonio G. Souza[a], Ieda Maria Garcia dos Santos[a,*]

[a]*LTM, Departamento de Química, CCEN, Universidade Federal da Paraíba, 58059-900, João Pessoa, PB, Brazil*
[b]*LSR, Departamento de Tecnologia Mecânica, CT, Universidade Federal da Paraíba, 58059-900, João Pessoa, PB, Brazil*
[c]*CMDMC, Instituto de Química de Araraquara, UNESP, 14800-900, Araraquara, SP, Brazil*
[d]*Departamento de Física, Universidade Federal de São Carlos, Caixa Posta 676, 13565-905, São Carlos, SP, Brazil*

Received 7 October 2005; received in revised form 12 December 2005; accepted 13 December 2005
Available online 2 February 2006

Abstract

In this work, the polymeric precursor method was used to obtain disordered Zn_2TiO_4 powders, either undoped or doped with Sn^{4+}, Cr^{3+} and V^{5+}, to be applied as photoluminescent material. The characterization was undertaken by means of thermal analysis (TG and DTA), X-ray diffraction (XRD), infrared spectroscopy (IR) and photoluminescence (PL). Previous works stated that titanate octahedra containing a short Ti–O distance show efficient luminescence at room temperature if these octahedra are isolated from each other. In the present work, the phenomenon was observed in condensed octahedra, sharing edges. The room temperature PL noticed in undoped Zn_2TiO_4 had its intensity increased by the dopant addition—the increase was of about 300% for V^{5+} doping, 400% for Cr^{3+} and 800% for Sn^{4+}.

Keywords: Disordered materials; Pechini; Luminescence; Titanate; Spinel

1. Introduction

Spinels have awakened great interest in crystallographic areas, particularly in the study of the physico-chemical properties of binary compounds and solid solutions [1]. Zinc titanate (Zn_2TiO_4) is an inverse spinel, which has been used as a catalyst and a pigment. In the catalysis area, different authors report the use of Zn_2TiO_4 as sorbent for removing sulfur from coal gasification product gases, in hot gas desulfurization units, at temperatures at the 400–700 °C range. Zinc titanate not only withstands these high temperatures, without meaningful zinc loss, but is also one of the leading regenerable catalysts [2–7]. As a dielectric material, zinc titanate was used as one of the components in dielectric compositions. Different authors have been studying their physical, electrical, and photoelectrochemical properties in order to investigate different applications [8,9].

Zinc titanate is usually synthesized by solid-state reaction, at high temperatures. When a temperature below 1000 °C is used, a long heat treatment is necessary [2–4,9]. Chemical synthesis methods were also employed—when co-precipitation method was used, a heat treatment at 700 °C for 2 h was used, but secondary phases were observed [7]; when citrate method was used, a heat treatment at 720 °C for 12 h was used. In this case, a single-phase material was obtained [6].

In the last decades, photoluminescence (PL) of crystalline materials was extensively studied. Recently, disordered and/or nanostructured materials with high photoluminescent emission in the visible region were evaluated, including titanium dioxide and titanates. These materials may substitute the crystalline compounds in many optical-electronic applications. Besides the advantage of their low synthesis temperature, their use is more convenient, once crystalline materials are photoluminescent only at

*Corresponding author. Fax: +55 83 3216 7441.
E-mail address: ieda@quimica.ufpb.br (I.M.G. Santos).

0022-4596/$ - see front matter © 2005 Elsevier Inc. All rights reserved.
doi:10.1016/j.jssc.2005.12.018

cryogenic temperatures, whereas disordered materials display PL at room temperature [10–17].

The chemical processing using solutions, including soft solution processing, has been attracting increased interest. Soft solution processing can be defined as an environmentally friendly processing, using aqueous solution. It also seems to provide results similar to every other process that uses fluids such as vapor [18], gas [19] and plasma or beam/vacuum processing [20], while consuming less total energy than other processing routes.

In the present study, the soft solution processing, the so-called polymeric precursor method [21–23], has been adopted for the synthesis of Zn_2TiO_4, with spinel structure, undoped and doped with Sn^{4+}, V^{5+} and Cr^{3+}. The crystal structure and photoluminescent properties were investigated.

2. Experimental

The reagents used in the synthesis were: citric acid (Vetec), ethylene glycol (Synth), zinc nitrate (Synth), tin citrate (prepared from tin chloride (Mallinckrodt) [24]), chromium III nitrate (Vetec), vanadium oxide (Aldrich) and titanium citrate (prepared from titanium isopropoxide (Hulls-Ag) [25]). The synthesis of the powder was performed using the polymeric precursor method, as described in Fig. 1.

A thermal analysis was carried out to evaluate the powder precursor decomposition. TG/DTA was performed by means of a TA Instrument, model SDT-2960. The analyses were done using approximately 20 mg of the powders, at a heating rate of 10 °C min^{-1} up to 700 °C, as previous analyses indicated that the material is stable above this temperature. A synthetic air atmosphere was used in order to simulate the furnace conditions and guarantee the carbon elimination.

The characterization by X-ray diffraction (XRD) and infrared spectroscopy (IR) was undertaken with samples heat treated at different temperatures. PL was evaluated after heat treatment at 300 °C.

The device used in the XRD was a Siemens diffractometer, model D-5000, with Cu$K\alpha$ radiation ($\lambda = 1.54056$ Å). The Rede 93 program, developed at the Chemistry Institute of Unesp, in Araraquara, Brazil, was used to calculate the lattice parameters [26]. Quartz was used as an external standard. The full-width at half-maximum (FWHM) of the (311) peaks was determined in order to evaluate the structural disorder. The crystallite sizes were calculated using Scherrer equation [27].

The IR spectra were recorded in a Bomem (FT-DA8) infrared spectrophotometer with KBr pellets in the 400–4000 cm^{-1} range.

The PL measurements were taken using a U1000 Jobin–Yvon double monochromator coupled to a cooled GaAs photomultiplier and a conventional photon-counting system. The 488.0 nm excitation wavelength of an argon-ion laser was used, with maximum output power of the laser kept at 20 mW. Previous works indicate a linear relation between the maximum emission peak wavelength ($\lambda_{Emission}$) and the exciting wavelength ($\lambda_{Exciting}$) [28]. As the 488.0 nm excitation wavelength has been used by other authors [13–16], it was chosen in order to compare PL in titanates with spinel structure with titanates with perovskite structure. All the measurements were taken at room temperature.

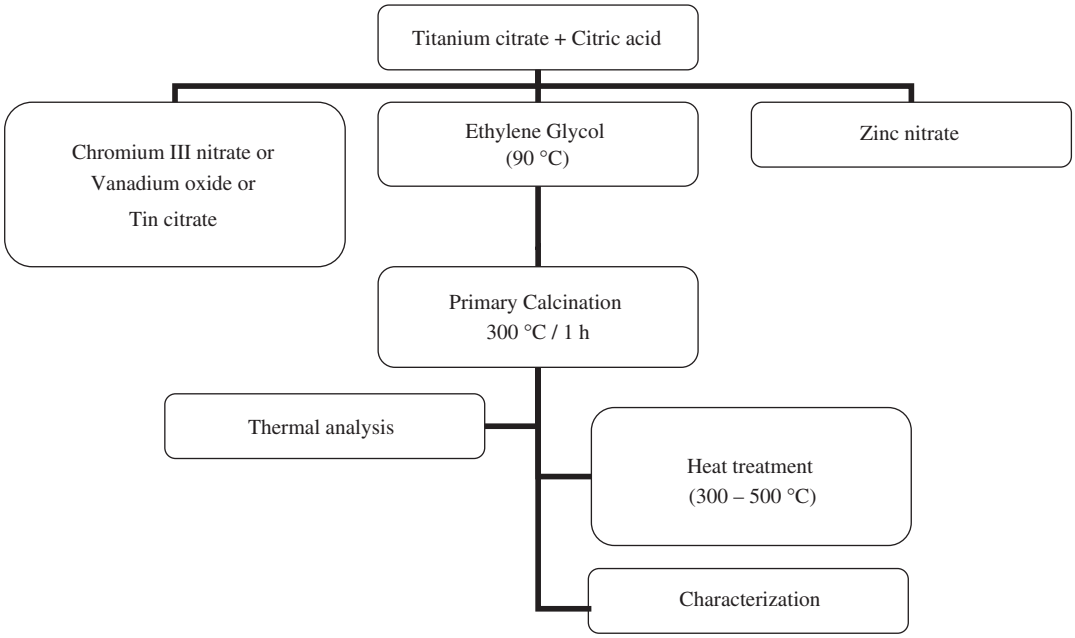

Fig. 1. Flow chart for the synthesis of $Zn_2Ti_{1-x}Me_xO_4$ ($Me = Cr^{3+}$, Sn^{4+} and V^{5+}, $x = 0$–1%) spinel.

3. Results and discussion

Thermogravimetric results (Fig. 2 and Table 1) indicate that all powder precursors present two thermal decomposition steps. The first step can be attributed to the loss of water and some gases adsorbed on the powder surface, at the 65–85 °C temperature range. The second step refers to organic matter decomposition, as well as to carboxyl groups bonded to metals, at the 215–500 °C temperature range. A reduction of mass loss after doping was observed.

DTA results indicate one endothermic peak, related to the loss of water, and one broad exothermic peak, related to organic matter decomposition. Samples doped with vanadium presented two exothermic peaks. Peak temperatures are presented in Table 1.

The differences in the DTA profiles may be related to the preferential sites occupied by the substitutional cation. In the case of V^{5+}, when zinc is present, VO_2^+ groups are formed, which hardly lead to compounds with σ(V–C) bonds [29]. This may conduce to segregation in the resin, with two decomposition steps.

Fig. 3 illustrates the spectra in the infrared region. Fig. 3a illustrates the powder precursor spectra after heat treatment at different temperatures. The powder precursor presents broad bands at about 460 cm^{-1}, related to the metal–oxygen stretching, and at 3425 cm^{-1}, related to water. It also presents a shoulder at 1600 cm^{-1} and well-defined bands at 1547 and 1390 cm^{-1}. The shoulder is characteristic of a ν(C = O) stretching mode for a unidentate complex, and the vibrations at 1547 and 1300 cm^{-1} are ascribed to the carboxyl stretching frequencies, ν(C = O) and ν(C–O), respectively, being related to a bidentate complex [25,30]. In the spectra, no bands related

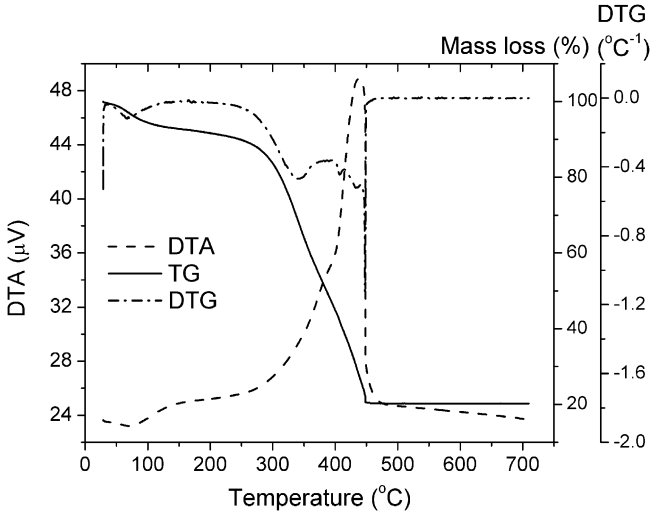

Fig. 2. Thermal analysis curves of the undoped Zn_2TiO_4 powder precursor.

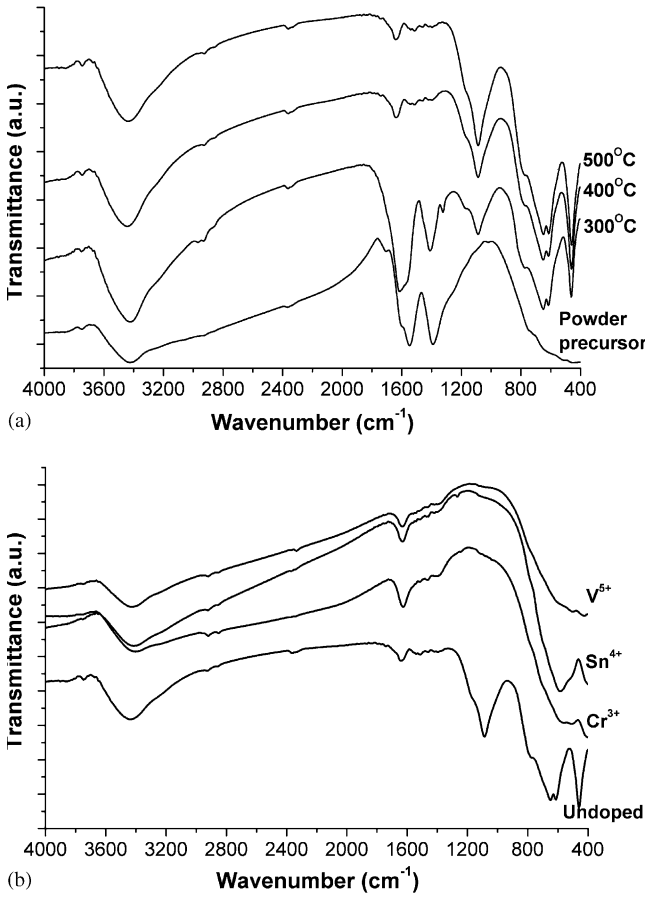

Fig. 3. (a) IR spectra of the Zn_2TiO_4 powder precursor, heat treated at different temperatures; (b) IR spectra of $Zn_2Ti_{0.99}Me_{0.01}O_4$ ($Me = Cr^{3+}$, Sn^{4+} and V^{5+}), heat treated at 500 °C.

Table 1
TG/DTA results of the thermal decomposition of the powder precursors

Samples	TG—second stage			DTA (°C)		Mass loss (%)
	T_i (°C)[a]	T_f (°C)[b]	T_p (°C)[c]	First peak	Second peak	
Zn_2TiO_4	227	460	341, 406, 433, 448	438		70
$Zn_{1.99}TiCr_{0.01}O_4$	240	447	336, 407, 445	439		69
$Zn_{1.99}TiSn_{0.01}O_4$	269	455	336, 367, 400	377		63
$Zn_{1.99}TiV_{0.01}O_4$	263	463	338, 356, 405, 415, 422	354	422	62

[a]Onset of decomposition temperature.
[b]Final decomposition temperature.
[c]Peak temperature, according to DTG curve.

to ester groups are observed, indicating that it has already been decomposed, during the primary calcinations [31].

After heat treatment of the powder precursor, the intensity of the carboxylate bands related to bidentate complex (1638 cm^{-1}) decreases more than the unidentate ones (~1550 and 1410 cm^{-1}), indicating that bidentate bonds are broken more easily than unidentate ones. For samples heat treated between 300 and 500 °C, bands at 461, 615, 650, 770 (shoulder), 1088 and 3440 cm^{-1} are also observed.

The bands at 1088 and 3440 cm^{-1} are related to the presence of C–OH. The band at 3440 cm^{-1} is assigned to the axial stretching of O–H, more specifically, to the hydrogen bonds among polymer molecules. The band at 1088 cm^{-1} is assigned to the axial stretching of C–O, coupled to the stretching of an adjacent C–C bond [32].

The bands at 461, 615, 650 and 770 (shoulder) cm^{-1} are attributed to the oxygen–metal linkage. The application of group theory to a rhombohedral spinel leads to the conclusion that four modes only are i.r. active. These four modes may be classified in two groups: the two modes having the highest frequencies, v_1 and v_2, are due to the motion of oxygen with respect to the cations; the two low frequency modes, v_3 and v_4, must be related to the displacements of the metallic cations. Moreover, if the cation masses and the electronic structures are not too widely different, the valency state is generally the most important factor determining the cation–oxygen bonding force, and the corresponding vibrational frequency. In the present case, only the high-frequency bands were evaluated [33]. As Zn_2TiO_4 is an inverse spinel, bands related to [TiO_6], [ZnO_6] and (ZnO_4) are expected. The absorption range of condensed [TiO_6] octahedral groups occurs at 650–550 cm^{-1}, and the absorption range of isolated (ZnO_4) tetrahedral groups occurs at 500–400 cm^{-1} [33].

Fig. 3b illustrates the spectra of the undoped and doped powder precursors calcined at 500 °C, in which a change in the spectra profile is observed. While the undoped sample presents well-defined bands at 770, 650, 610 and 458 cm^{-1}, doped samples present broad bands. The V-doped sample presents a broad band in the range 710–400 cm^{-1}, the Cr-doped sample also presents a broad band in this region, but a well-defined band starts at about 400 cm^{-1}, the Sn-doped sample presents a band at 585 cm^{-1} and another well-defined band starts at about 400 cm^{-1}. The partial loss of order and a random cation distribution could account for the loss of resolution in the spectra [34]. An important point is the decrease in the C–OH bond, indicated by the disappearance of the band at 1088 cm^{-1}.

Fig. 4 illustrates the diffraction patterns of the Zn_2TiO_4 doped with Cr^{3+}, Sn^{4+} and V^{5+}, heat treated at 500 °C. The spinel phase can be observed. When V^{5+} cations are introduced, secondary phases are formed. As it is difficult for V^{5+} to be introduced into the Zn_2TiO_4 lattice, due to its coordination, segregation occurs in the resin, leading to the formation of secondary phases (ZnO and $ZnTiO_3$).

Using the REDE 93 program, the unit cell volume was determined. According to JCPDS files, the unit cell volume of the Zn_2TiO_4 phase is 605.5 $Å^3$. In the present study, a smaller unit cell volume was obtained (601.2 $Å^3$), probably due to the smaller amount of defects in the structure, which is characteristic of the polymeric precursor method.

The results of the unit cell volume are presented in Fig. 5. For the doping with chromium and tin, an increase in the unit cell volume with the dopant amount is observed, whereas in the case of vanadium a decrease occurs. This behavior is related to the distortion caused by each dopant

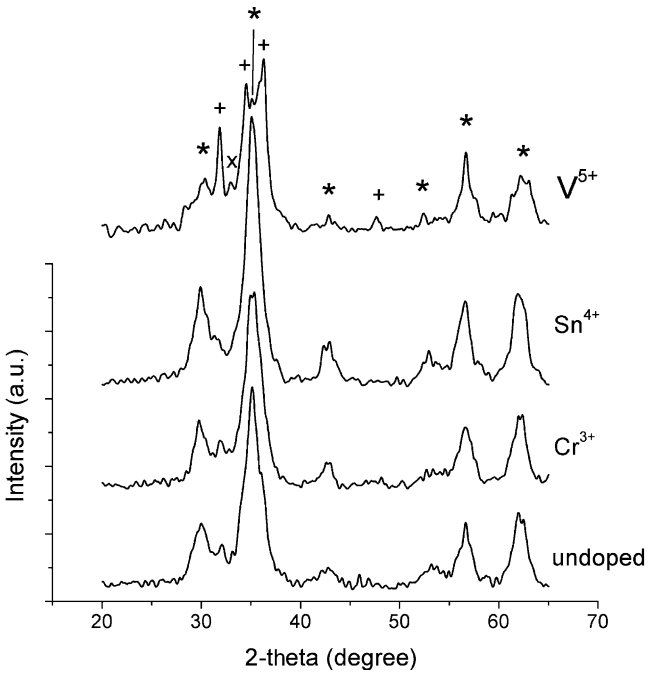

Fig. 4. XRD patterns of $Zn_2Ti_{0.99}Me_{0.01}O_4$ ($Me = Cr^{3+}$, Sn^{4+} and V^{5+}), heat treated at 500 °C. *, Zn_2TiO_4; +, ZnO; ×, $ZnTiO_3$.

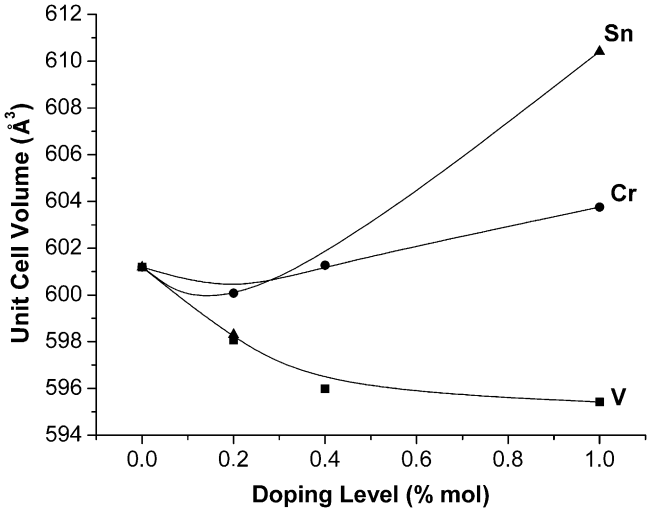

Fig. 5. Unit cell volume of $Zn_2Ti_{1-x}Me_xO_4$ ($Me = Cr^{3+}$, Sn^{4+} and V^{5+}, $x = 0$–1%), heat treated at 500 °C.

in the octahedral sites. In relation to vanadium, the decrease in unit cell volume indicates that, in spite of the difficulty of its introduction into the unit cell, some vanadium ions succeed in doing so.

Fig. 6a shows FWHM of the Zn_2TiO_4 doped with 1 mol% of Cr^{3+}, Sn^{4+} and V^{5+}, heat treated at 400 and 500 °C. After calcinations at 400 °C, the results indicate a decrease in FWHM with doping, pointing out to a lower degree of disorder—this disorder decrease may be due to an increase in crystallite size and/or due to a lower internal stress.

After heat treatment at 500 °C, the variation of FWHM is smaller. The (311) peak of the Cr-doped sample presents the same FWHM of the undoped sample, while both the V- and Sn-doped samples display a smaller value. These results are in agreement with the unit cell volume measurements, which indicate that chromium addition leads to the smallest change in the lattice parameters.

Crystallite size results, Fig. 6b, indicate that the change in FWHM is strictly related to crystallite growth, once the graphics present the same profile. Therefore, the IR and XRD results indicate that the doping leads to an increase in short-range disorder, but increases the diffusion rate, increasing crystallite size and, consequently, decreasing surface defects. Chromium doping leads to the smallest change in structure.

In relation to the doping level (Fig. 6c), it may be observed that samples doped with smaller amounts (0.1–0.4 mol%) of Sn^{4+} or Cr^{3+} present higher crystallite sizes than samples doped with 1 mol%. At small doping levels, similar sizes were obtained, whereas for 1 mol%, tin-doped samples present higher crystallite size than the chromium-doped samples. This result indicates that chromium doping also leads to the smallest changes in morphology.

The PL results (Figs. 7a, 7b and 7c) indicate that disordered titanates with spinel structure present high luminescence, especially when the dopants are introduced within the structure [16]. This is probably due to the increase in short-range disorder, as indicated by the infrared results. This result is in agreement with the literature, as it will be discussed as follows. It should be emphasized that 1 mol% of chromium doping, which leads to the smallest change in spinel structure, leads to the smallest increase in PL (Fig. 7b).

Bouma and Blasse studied the PL in crystalline titanates and concluded that titanate octahedra containing a short Ti–O distance show efficient luminescence at room temperature, if these octahedra are isolated from each other [10]. In the present case, PL is observed in an amorphous titanate, in which the coordination octahedral share edges, instead of corners, a characteristic of the spinel structure of the space group *Fd*3*m* [35]. PL in $Li_2ZnTi_3O_8$ spinel has already been observed, as presented by Câmara et al. [36]. In their work, the spinel of the space group *P*4332 was evaluated and the authors concluded that PL depends on the degree of the system disordering, which

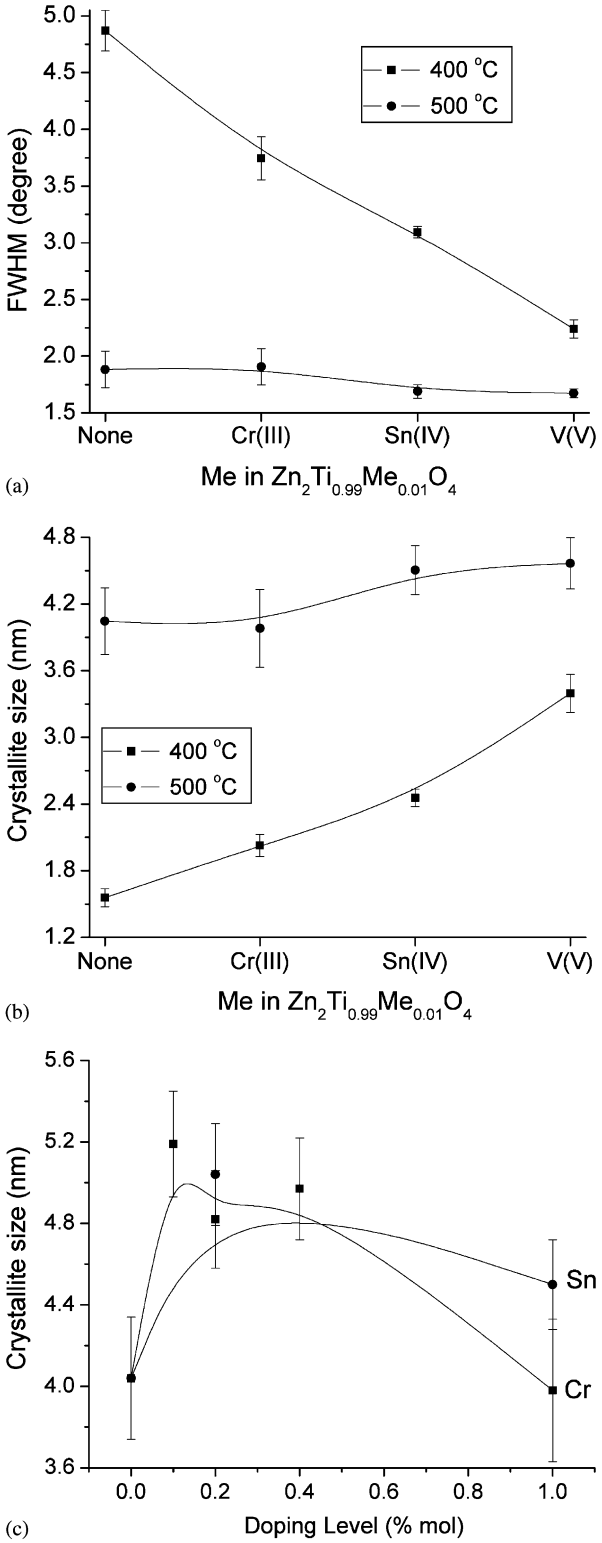

Fig. 6. Evaluation of XRD results of $Zn_2Ti_{0.99}Me_{0.01}O_4$ ($Me = Cr^{3+}$, Sn^{4+} and V^{5+}) as a function of doping. (a) FWHM; (b) crystallite size of samples, with 1 mol% of dopant, heat treated at different temperatures; (c) crystallite size of samples with different dopant amounts, heat treated at 500 °C.

leads to the appearance of new energy levels, both in the valence band and in the conduction band, decreasing the band gap. In the present case, besides the low synthesis

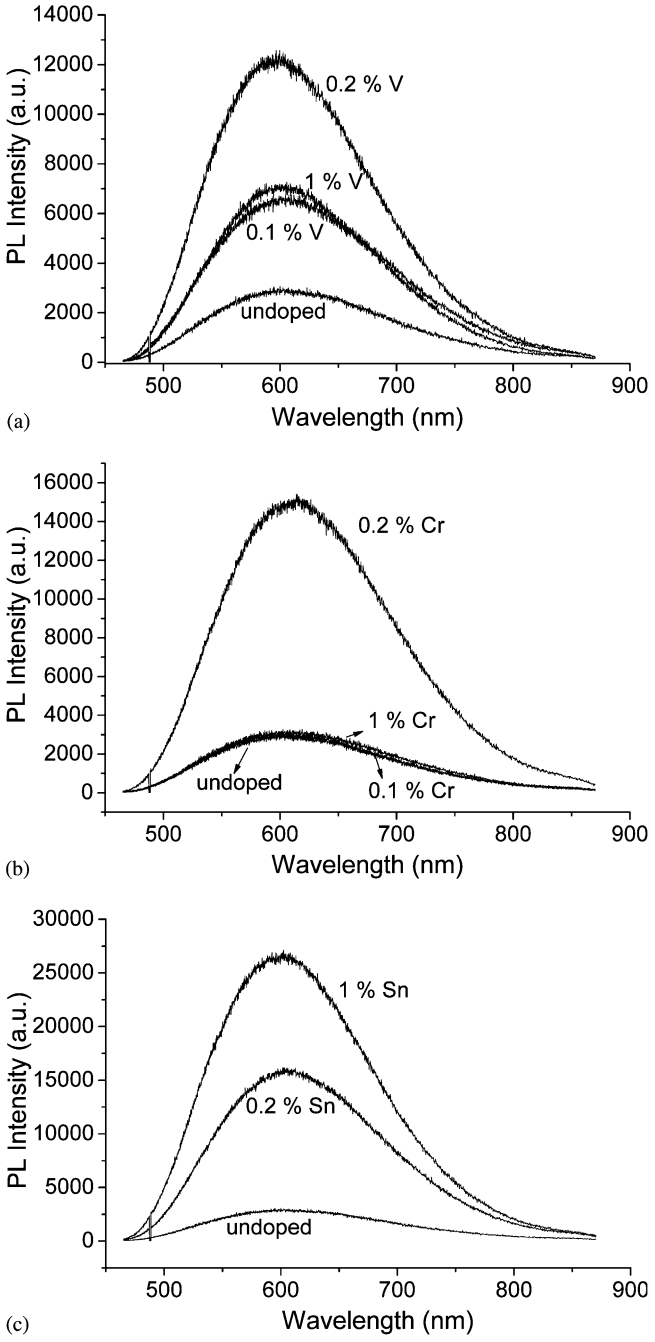

Fig. 7. PL spectra of $Zn_2Ti_{1-x}Me_xO_4$ ($Me = Cr^{3+}$, Sn^{4+} and V^{5+}, $x = 0$–1%), heat treated at 300 °C. (a) Vanadium; (b) chromium; (c) tin.

temperature, doping is also used to increase the disorder degree.

Deconvolution of the PL spectra of all samples (Fig. 8) showed four peaks. The results extracted from the deconvolution spectra are presented in Table 2. The fourth peak was not considered due to its high width and low intensity. PL quantum efficiency (PLQ) was evaluated from the integrated area under the peaks [37,38].

The results indicate a small tendency of decrease in the energy of all three peaks, when the dopant is added to Zn_2TiO_4. The highest decrease is observed for chromium doping, while no meaningful change is noted for vanadium. This result may be related to a decrease in the band gap due to the creation of defects in the structure [1].

As explained by Blasse and Grabmaier [39], the PL arises from a radiative return to the ground state, a phenomenon that is in concurrence with the non-radiative return to the ground state, in which the energy of the excited state is used to excite the vibrations of the host lattice, i.e. to heat the lattice. The radiative emission process occurs more easily if trapped holes or trapped electrons exist in the structure.

The literature results of PL in amorphous titanates indicate that the phenomenon is related to the presence of $[TiO_5]$ clusters, leading to delocalized electronic levels in the optical gap. Studies of different titanates showed that the visible PL emission in amorphous material is directly related to the exponential optical edges and tails. The nature of these exponential optical edges and tails may be associated to defects promoted by the disordered structure of the amorphous material [14–17].

The XANES studies on $SrTiO_3$ pointed out that disordered titanates synthesized using a soft chemical processing are formed basically by sixfold oxygen–Ti coordination (TiO_6—octahedra) and fivefold oxygen–Ti coordination (TiO_5—square-base pyramids) [40].

Recently, Orhan et al. evaluated the PL in $SrTiO_3$ and stated that two main and connected factors are responsible for the PL behavior of SrO-deficient $Sr_{1-x}TiO_{3-x}$: (i) localized electronic levels induced in the valence band by the symmetry-breaking process ongoing from stoichiometric to Sr-deficient $Sr_{1-x}TiO_{3-x}$, and (ii) the coexistence of both $[TiO_6]$ and $[TiO_4]$ cluster configurations in the deficient $Sr_{1-x}TiO_{3-x}$ structure, yielding a charge imbalance that encourages the trapping of holes in the previously mentioned localized states [13].

In relation to quantum efficiency (Table 2), tin doping led to the highest PLQ, for all transitions, in all doping amounts. In all samples, the maximum PLQ was observed in the second peak (2.050–2.095 eV). For chromium and vanadium, the addition of 1 mol% of the dopant leads to the decrease in PLQ.

Depending on the ligand field energy, dopant addition can lead to intermediate electronic levels, making electron transition easier. Different behaviors are observed according to the dopant. For Cr^{3+} and V^{5+}, ionic or electronic defects are probably created, according to Eqs. (1)–(4). For Sn^{4+}, these defects are not created.

$$Cr_2O_3 \xrightarrow{Zn_2TiO_4} 2Cr'_{Ti} + V_O^{\bullet\bullet} + 3O_O^x \quad (1)$$

$$Cr_2O_3 \xrightarrow{Zn_2TiO_4} 2Cr'_{Ti} + 2h^{\bullet} + 3O_O^x \quad (2)$$

$$V_2O_5 \xrightarrow{Zn_2TiO_4} 2V_{Ti}^{\bullet} + V''_{Zn} + 5O_O^x \quad (3)$$

$$V_2O_5 \xrightarrow{Zn_2TiO_4} 2V_{Ti}^{\bullet} + 2e' + 5O_O^x \quad (4)$$

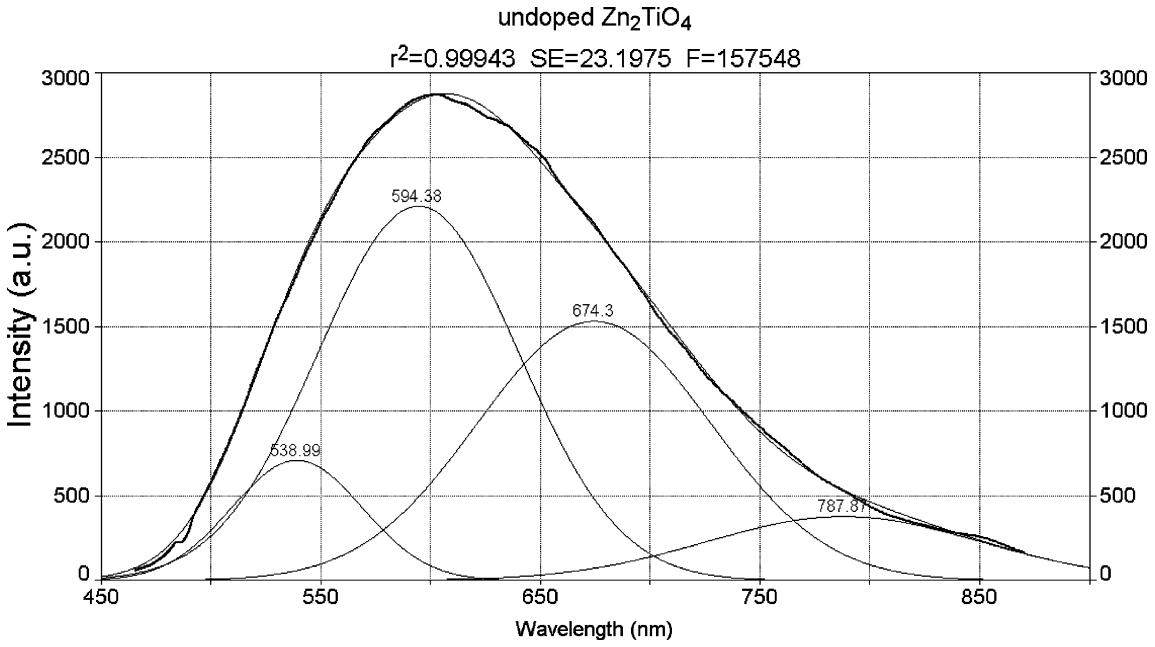

Fig. 8. Deconvolution of the PL spectrum of Zn_2TiO_4, heat treated at 300 °C.

Table 2
PL peak energy and quantum efficiency (PLQ) of the different transitions, extracted from the deconvoluted spectra of the doped and undoped Zn_2TiO_4

Sample	Peak 1		Peak 2		Peak 3	
	Energy (eV)	PLQ	Energy (eV)	PLQ	Energy (eV)	PLQ
Zn_2TiO_4	2.301±0.004	1.1	2.088±0.014	2.4	1.840±0.016	2.0
$Zn_2Ti_{0.999}Cr_{0.001}O_4$	2.292±0.004	0.53	2.074±0.017	3.0	1.818±0.013	1.8
$Zn_2Ti_{0.998}Cr_{0.002}O_4$	2.267±0.004	3.2	2.056±0.014	13	1.832±0.016	9.4
$Zn_2Ti_{0.99}Cr_{0.01}O_4$	2.279±0.004	0.69	2.050±0.013	3.2	1.787±0.010	1.9
$Zn_2Ti_{0.998}Sn_{0.002}O_4$	2.279±0.004	3.1	2.067±0.010	14	1.832±0.013	9.4
$Zn_2Ti_{0.99}Sn_{0.01}O_4$	2.288±0.004	5.6	2.056±0.007	28	1.813±0.005	8.3
$Zn_2Ti_{0.999}V_{0.001}O_4$	2.288±0.004	1.5	2.067±0.010	5.9	1.826±0.013	3.8
$Zn_2Ti_{0.998}V_{0.002}O_4$	2.292±0.004	2.2	2.081±0.010	12	1.832±0.011	5.7
$Zn_2Ti_{0.99}V_{0.01}O_4$	2.301±0.004	1.1	2.095±0.007	6.1	1.854±0.008	4.3

The lower PL intensity of the samples doped with Cr^{3+} and V^{5+}, compared with the Sn^{4+} samples, is probably due to the charge polarization in the structure. According to Diallo et al. [41], several electronic defects are undesirable because their presence in the material, even at low concentration, can contribute to quench the luminescence.

It should be emphasized that, in spite of the vanadium segregation, its presence increases the PL intensity.

For tin, the decrease in luminescent emission, noticed for higher doping levels, is not observed. This probably occurs because Sn^{4+} substitutes Ti^{4+}, leading to a disorder in the lattice, without formation of electronic or ionic defects. Thus, more tin may be added to the structure.

4. Conclusions

Zinc titanate, doped with chromium or tin, is single phase, while vanadium doping leads to secondary phases. In spite of this, a change in the lattice parameters indicates that some vanadium succeeds in being introduced into the Zn_2TiO_4 lattice. It was observed that doping leads to an increase in short-range disorder and to an increase in crystallite size. Chromium doping leads to the smallest change.

PL results indicate a high emission when dopants are added, probably associated to short-range disorder. Tin doping leads to the highest photoluminescent emission. For chromium and vanadium, ionic or electronic defects probably lead to charge polarization, decreasing the luminescent emission, when higher dopant amounts are added.

Acknowledgments

The authors gratefully acknowledge the financial support of the Brazilian agencies CNPq/PRONEX, CNPq/PADCT, CAPES and FAPESP/CEPID.

References

[1] Y.-M. Chiang, D.P. Birnie III, W.D. Kingery, Physical Ceramics—Principles for Ceramic Science and Engineering, Wiley, New York, 1997.
[2] H.K. Jun, T.J. Lee, S.O. Ryu, J.C. Kim, Ind. Eng. Chem. Res. 40 (2001) 3547–3556.
[3] M. Pineda, J.L.G. Fierro, J.M. Palacios, C. Cilleruelo, E. García, J.V. Ibarra, Appl. Surf. Sci. 119 (1997) 1–10.
[4] L. Alonso, J.M. Palacios, R. Moliner, Energy Fuel 15 (2001) 1396–1402.
[5] R.B. Slimane, J. Abbasian, Adv. Environ. Res. 4 (2000) 147–162.
[6] S. Lew, A.F. Sarofim, M. Flytzani-Stephanopoulos, Chem. Eng. Sci. 47 (1992) 1421–1431.
[7] K. Jothimurugesan, S.K. Gangwal, Ind. Eng. Chem. Res. 37 (1998) 1929–1933.
[8] K.H. Yoon, J. Cho, D.H. Kang, Mater. Res. Bull. 34 (1999) 1451–1461.
[9] H.T. Kim, J.D. Byun, Y. Kim, Mater. Res. Bull. 33 (1998) 963–973.
[10] B. Bouma, G. Blasse, J. Phys. Chem. Solids 56 (1995) 261–265.
[11] Y. Zhu, C. Ding, G. Ma, Z. Du, J. Solid State Chem. 139 (1998) 124–127.
[12] W.F. Zhang, M.S. Zhang, Z. Yin, Q. Chen, Appl. Phys. B 70 (2000) 261–265.
[13] E. Orhan, F.M. Pontes, M.A. Santos, E.R. Leite, A. Beltran, J. Andrés, T.M. Boschi, P.S. Pizani, J.A. Varela, C.A. Taft, E. Longo, J. Phys. Chem. B 108 (2004) 9221–9227.
[14] C.D. Pinheiro, E. Longo, E.R. Leite, F.M. Pontes, R. Magnani, J.A. Varela, P.S. Pizanni, T.M. Boschi, F. Lanciotti, Appl. Phys. A—Mater. 77 (2003) 81–85.
[15] F.M. Pontes, C.D. Pinheiro, E. Longo, E.R. Leite, S.R. de Lazaro, R. Magnani, P.S. Pizani, T.M. Boschi, F. Lanciotti, J. Lumin. 104 (2003) 175–185.
[16] D.M.A. Melo, A. César, A.E. Martinelli, Z.R. Silva, E.R. Leite, E. Longo, P.S. Pizanni, J. Solid State Chem. 177 (2004) 670–674.
[17] P.R. de Lucena, F.M. Pontes, C.D. Pinheiro, E. Longo, P.S. Pizani, S. Lázaro, A.G. Souza, I.M.G. dos Santos, Cerâmica 50 (2004) 138–144.
[18] J. Garapon, B. Poumellec, S. Vacher, A.N. Trukhin, J. Non-Cryst. Solids 311 (2002) 83–88.
[19] M. Zhang, J. Yu, W. Chen, Z. Yin, Prog. Cryst. Growth Ch. 40 (2000) 33–42.
[20] J.S. Kang, H.S. Kang, S.S. Pang, E.S. Shim, S.Y. Lee, Thin Solid Films 443 (2003) 5–8.
[21] P.A. Lessing, Am. Ceram. Soc. Bull. 68 (1989) 1002.
[22] M. Kakihana, T. Okubo, M. Arima, Y. Nakamura, M. Yashima, M. Yoshimura, J. Sol-Gel Sci. Techn. 12 (1998) 95.
[23] S.C. Souza, I.M.G. Santos, M.R.S. Silva, M.R. Cássia-Santos, L.E.B. Soledade, A.G. Souza, S.J.G. Lima, E. Longo, J. Therm. Anal. Calorim. 79 (2005) 451–454.
[24] M.M. Besso, US Patent no. 3,213,120, 1965.
[25] E.R. Leite, C.M.G. Sousa, E. Longo, J.A. Varela, Ceram. Int. 21 (1995) 143–152.
[26] C.O. Paiva-Santos, D. Garcia, I.P. Mascarenhas, J.A. Eiras, Cerâmica 35 (1989) 153.
[27] B.D. Cullity, Elements of X-ray Diffraction, Addison-Wesley Publishing Company, Massachusetts, 1967.
[28] E.R. Leite, F.M. Pontes, E.J.H. Lee, R. Aguiar, E. Longo, D.S.L. Pontes, M.S.J. Nunes, H.R. Macedo, P.S. Pizani, F. Lanciotti Jr, T.M. Boschi, J.A. Varela, C.A. Paskocimas, Appl. Phys. A 74 (2002) 529–532.
[29] J.D. Lee, Concise Inorganic Chemistry, fourth ed., Chapman & Hall, New York, 1991.
[30] K. Nakamoto, Infrared and Raman Spectra of Inorganic and Coordination Compounds, fourth ed., Wiley, New York, 1986.
[31] P. Duran, D. Guterrez, J. Tartaj, A. Banares, C. Moure, J. Eur. Ceram. Soc. 22 (2002) 797–807.
[32] R.M. Silverstein, F.X. Webster, Spectrometric Identification of Organic Compounds, sixth ed., Wiley, New York, 1998.
[33] J. Preudhomme, P. Tarte, Spectrochim. Acta A 27 (1971) 961–968.
[34] R. Alcantara, M. Jaraba, P. Lavela, J.L. Tirado. Ph. Biensan, A. de Guibert, C. Jordy, J. P. Peres. Chem. Mater. 15 (2003) 2376–2382.
[35] Hk. Müller-Buschbaum, J. Alloys Compd. 349 (2003) 49–104.
[36] M.S.C. Câmara, M.F.C. Gurgel, S.R. Lazaro, T.M. Boschi, P.S. Pizani, E.R. Leite, A. Beltran, E. Longo, Int. J. Quantum Chem. 103 (2005) 580–587.
[37] T. Tiedje, B. Abeles, B.G. Brooks, Phys. Rev. Lett. 54 (1985) 2545–2548.
[38] K.V. Adarsh, K.S. Sangunni, S. Kokenyesi, I. Ivan, M. Shipljak, J. Appl. Phys. 97 (2005) 044314/1–044314/5.
[39] G. Blasse, B.C. Grabmaier, Luminesc. Mater., Springer, Berlin Heildlbery, 1994.
[40] F.M. Pontes, E. Longo, E.R. Leite, E.J.H. Lee, J.A. Varela, P.S. Pizani, C.E.M. Campos, F. Lanciotti, V. Mastellaro, C.D. Pinheiro, Mater. Chem. Phys. 77 (2002) 598–602.
[41] P.T. Diallo, K. Jeanlouis, P. Boutinaud, R. Mahiou, J.C. Cousseins, J. Alloys Compd. 323–324 (2001) 218–222.